

Study of *n*-Butane Isomerization on Acid Catalysts Niobium and Lanthanum Promoted Tungstated Zirconia: *n*-Butane Isomerization Activity

Z. Mohamed Seghir,^{a*} M. Djennad,^a R. Schomäcker,^b and M. R. Ghezzar^c

This work is licensed under a Creative Commons Attribution 4.0 International License



^aLaboratory of Structure, Elaboration and Application of Molecular Materials, SEA2M Department of Process Engineering, University Abdelhamid Ibn Badis, Mostaganem, Algeria

^bDepartment of Chemistry, Technical University Berlin, Straße des 17. Juni 124, 10 623 Berlin, Germany

^cLaboratory of Science and Technical Environment and Valorization, Department of Process Engineering, University Abdelhamid Ibn Badis, Mostaganem, Algeria

Abstract

The requirement for environmentally friendly catalysts for the isomerization of alkanes has prompted research on the tungstate-zirconia (WZ) system. The present work examines the activity and selectivity of lanthanum (La) promoted tungstate-zirconia (LWZ) and niobium (Nb) promoted tungstate-zirconia (NWZ) catalysts. In this study, 1 % La promoted WZ (1 % LWZ) and 1 % Nb promoted WZ (1 % NWZ) catalysts were investigated in isomerization of *n*-butane in the presence of hydrogen. The studied catalysts were characterized by different methods: nitrogen physisorption, temperature programmed desorption of NH₃, thermogravimetric analysis, and X-ray diffraction. The catalytic activity and selectivity were significantly improved by the addition of 1 % Nb. The redox process in the Nb-containing catalyst (1 % NWZ) played a central role by providing the highest acidic sites (283.53 μmol g⁻¹) with appropriate activation energies for the skeletal rearrangement of the reactant (*n*-butane). Furthermore, this study highlights the determining role of the transfer process of adsorbed species from ZrO₂ to W as well as to the Nb environment. The conversion of *n*-butane (27.34 %) and the selectivity to *i*-butane (92.34 %) for NWZ were significantly higher than WZ and LWZ catalysts. The experimental results revealed that Nb was a more effective promoter than La.

Keywords

Tungstated zirconia, *n*-butane isomerization, niobium, lanthanum, acidity

1 Introduction

Skeletal isomerization of *n*-butane has of particular interest in the ultimate petroleum refining industry in producing hydrocarbons of high octane number. The reaction product (isobutene) is the precursor for the synthesis of MTBE, ETBE, isoprenes, polyisobutene, *tert*-butyl alcohol, etc.¹ Therefore, the interest in developing more efficient and cost-effective commercial processes for direct isomerization of *n*-butane and other light alkanes has increased in recent years.^{2–5} Isomerization reaction is generally realized on (strong) acid solids in order to lower the reaction temperature of the skeletal isomerization reaction of light alkanes.^{6,7}

The best known catalysts for light *n*-alkanes isomerization at the commercial scale are Pt on chlorinated alumina or Pt/H-mordenite.^{8,10,11} Pt on chlorinated alumina has high catalytic activity and selectivity to branched isomers at low temperature (115–150 °C). However, this type of catalyst suffers from its chlorine contents, and as such is subjected to stringent environmental control. Pt/H-mordenite does not have these disadvantages, but it requires higher reaction temperature (260 °C), which is thermodynamically unfavourable for the formation of branched isomers.

On the other hand, *Hino et al.*¹² and *Xu Yan et al.*¹³ claimed that sulphated zirconia (SZ) is active for *n*-butane isomerization at room temperature. In addition, the activity, selectivity, and stability of SZ can also be improved by adding noble metals and transition metal oxides such as those of iron and manganese, as reported by *Yamaguchi*,⁹ *Tanabe et al.*¹⁴, *Loften et al.*¹⁸ and *Wang et al.*¹⁹

Non-promoted and promoted SZ are active for alkanes isomerization but suffer from main drawback such as deactivation, which can be very rapid, by poisoning of the noble metal function with sulphur species formed by sulphate groups in reducing atmospheres.^{20,21}

The works of *Hino et al.*⁷ on tungsten oxide supported on zirconia catalysts used for the skeletal isomerization of alkanes, showed that super-acid sites are created by interaction of amorphous WO₃ with ZrO₂ during the formation of tetragonal crystalline structure in ZrO₂. Addition of platinum and transition metal oxides (Ga, Al) greatly improved the catalytic activity of tungstate-zirconia (WZ). The two latter have shown good activity and selectivity for *n*-butane isomerization, Ga was a more efficient promoter with good catalytic performances compared to Al, as reported by *Xiao-Rong et al.*²⁴ It is clear that the activity and selectivity of *n*-alkanes isomerization depend strongly not only on the strength of the acids sites but also their distributions. The Brønsted acid site strength on ZrO₂ depends on the WO₃ loading. As reported by *Scheithauer et al.*²⁵, higher

* Corresponding author: Zahira Mohamed Seghir, PhD
Email: zahira.mohamedseghir@univ-mosta.dz

WO₃ loading results in a higher concentration of permanent Brønsted acid sites, and thus higher catalyst activity. Similarly, Naito et al.²⁶ have suggested that the permanent Brønsted acid sites on monolayer dispersed WO₃ are active for the isomerization of *n*-butane.

Furthermore, it has been shown by De Rossi et al.²⁷ that for isomerization activity development, WZ catalysts should be prepared from amorphous hydrous zirconia and then activated at high temperature (600–900 °C).

In the present work, interest was focused toward the study of the promotion effect of La³⁺ and Nb⁵⁺ when added to WZ for their potential role as active and selective catalysts for the isomerization of *n*-butane.

2 Material and methods

2.1 Catalysts preparation

Tungsten-zirconia oxide catalyst was prepared by wet impregnation of commercial zirconium hydroxide Zr(OH)₄ (from Aldrich 97 %) using ammonium metatungstate (NH₄)₆W₁₂O₄₀ · *n*H₂O (from Fluka) (used as precursor) solutions in a large excess of water with concentrations adjusted in order to obtain 15 wt% WO₃. After drying overnight at 110 °C, the impregnated samples were calcined in air at 800 °C for 3 h as indicated in Arata.²⁸

In the calculation of a theoretical monolayer of WO₃, it was assumed that one WO₃ molecule occupied 23 Å², as reported by Wang et al.²⁰

Nb-promoted (1 % NWZ) and La-promoted (1 % LWZ) catalysts were obtained by impregnating dispersed WO₃/ZrO₂ (WZ, yellow) in C₄H₄NNbO₈ · H₂O and La (NO₃)₂ · *n*H₂O aqueous solutions using dry impregnation method (Incipient wetness impregnation), then oven dried at 110 °C for 24 h. Adjustments of solution concentrations were performed in order to obtain 1 % by wt for both Nb and La on the synthesized catalysts. The promoted solids were then heated in air at 650 °C for 3 h.

2.2 Catalysts characterisation

2.2.1 Powder XRD

X-ray diffraction patterns were recorded on a X'Pert MPD Pro (PANalytical B.V, Almelo, Netherlands) diffractometer fitted with Bragg-Brentano geometry using CuK_α radiation (λ = 1.5418 nm) in the 2θ range 10°–80° at a scan speed of 0.5° min⁻¹. The catalysts were prepared using a commercial sample holder, which was a circle hollowed out on the surface (silicon zero background sample holder).

2.2.2 Thermogravimetric analysis

The thermogravimetric analysis (TG-DTA) of the catalyst samples was performed on a NETZSCH Proteus. The experiments were carried out at a heating rate of 10 °C min⁻¹ from 25 to 900 °C in nitrogen flow rate of 60 ml min⁻¹.

2.2.3 Adsorption – desorption isotherms (BET analysis)

The BET surface area (*S*_{BET}) of the solids was measured from nitrogen physisorption at –197 °C (or 76 K) using a Quantachrome Autosorb 1 instrument. The samples were previously degassed under dynamic vacuum conditions for 1 h at 200 °C. The specific surface areas were calculated from desorption isotherms using the BET equation, while the pore structure parameters were determined by the BJH method.

2.2.4 NH₃-temperature programmed desorption (NH₃-TPD)

NH₃-TPD experiments were carried out to determine the total acidity and the acidic strength distribution of catalysts. Catalyst was activated under hydrogen flow at 400 °C for 3 h, and then cooled to room temperature under the nitrogen atmosphere. Ammonia was introduced at 100 °C, followed by purge with nitrogen at the same temperature for 2 h. The TPD profiles were recorded by raising the temperature to 600 °C at a constant rate (10 °C min⁻¹) under nitrogen flow using a TCD detector.

2.2.5 Catalytic measurements

Catalytic measurements were carried out in a fixed bed flow reactor operated under isothermal conditions at atmospheric pressure. Prior to reaction, catalysts (1 g of 40–80 mesh sieved) were systematically pre-treated under air at 450 °C and maintained at this temperature for 3 h under air, and then flushed under hydrogen flow at reaction temperature for 1 h. The isomerization of *n*-butane was performed at 300 °C at volumetric rate of a mixture of 3 ml min⁻¹ of *n*-butane and 18 ml min⁻¹ of H₂.

Online gas analyses of reactants and products were carried out by Shimadzu gas chromatograph (GC-2014), and then respective amounts deduced for the calculation of catalytic activity and selectivity.

3 Results and discussion

The impregnated catalysts contained about 14–15 wt% of W metal. These loadings were almost similar to the theoretical monolayer capacity of ZrO₂ (7.3 W nm⁻²), which is equivalent to about 12–13 wt% of W, as reported by Barton et al.²⁹ The La and Nb contents were 1 wt% and the freshly prepared catalysts were yellowish in colour.

XRD patterns of WZ promoted with 1 % La and 1 % Nb catalysts are presented in Fig. 1.

Peaks have been assigned according to Vaudagna et al.³⁰ and Chen et al.³² Like sulphate promotion, the addition of tungsten oxide stabilizes the tetragonal phase of zirconia, delaying the transformation of this metastable phase into a thermodynamically stable phase. WZ samples exhibit similar behaviour since an amount of W (14–15 %) is required for inhibition of tetragonal transformation in monoclinic.

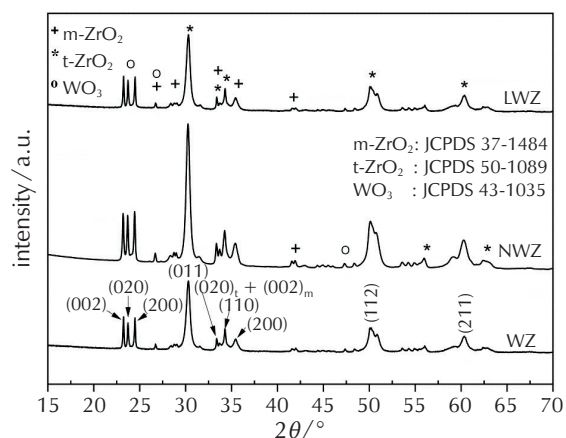


Fig. 1 – XRD patterns recorded for calcined WZ, 1 % NWZ, and 1 % LWZ catalysts

All samples present a mixture of a monoclinic and a tetragonal phase of zirconia in which the main peak appears at $2\theta = 30.2^\circ$. For all the diagrams, the group of peaks at 2θ ($23\text{--}25^\circ$) is attributed to the crystal structure of WO_3 . The most intense peaks characteristics of catalytic materials are identified by the Miller indices in Fig. 1.^{37,39} This result may indicate the existence of free tungstate anions on the catalyst surface forming WO_3 during calcination at high

temperature, as mentioned by *Boyse et al.*³³ and *Karima et al.*³⁴ These results are also in agreement with previous observations of *Larsen et al.*,³¹ *Vaidyanathan et al.*,³⁵ and *Iglesia et al.*³⁶ Previous studies^{38,40} have shown that WO_3 microcrystallites identified by reflections at 2θ ($23\text{--}25^\circ$) had developed on the zirconia surface at tungsten coverages above the monolayer as a result of the agglomeration of surface WO_x species. *Youri et al.*⁴¹ presumed that the amorphous WO_3 species with W octahedral coordination are responsible for the isomerization activity. *Huang et al.*⁴² reported that the tetragonal structure is essential in highly active acid catalysts and that a monoclinic phase would result in a significantly lower acidity. No peaks corresponding to niobium or lanthanum were observed in different diagrams, because of the lower concentration (1 %) of either Nb or La, which is below the detection limit of the X-ray equipment. Therefore, the promoters were so well dispersed that no crystallization forms appeared. Through the works of *Chen et al.*⁴³ and *Stichert et al.*⁴⁴ it was known that the tetragonal structure was essential in highly active acid catalysts, and that the monoclinic phase was poorly efficient in *n*-butane isomerization. This suggested that niobium and lanthanum influenced catalytic activity through the crystallization behaviour. They promoted the formation of the tetragonal phase and stabilized tetragonal zirconia crystallites at high calcination temperature.

The TG/DTA curves for the WZ, 1 % NWZ, and 1 % LWZ catalysts are shown in Fig. 2. The decomposition process

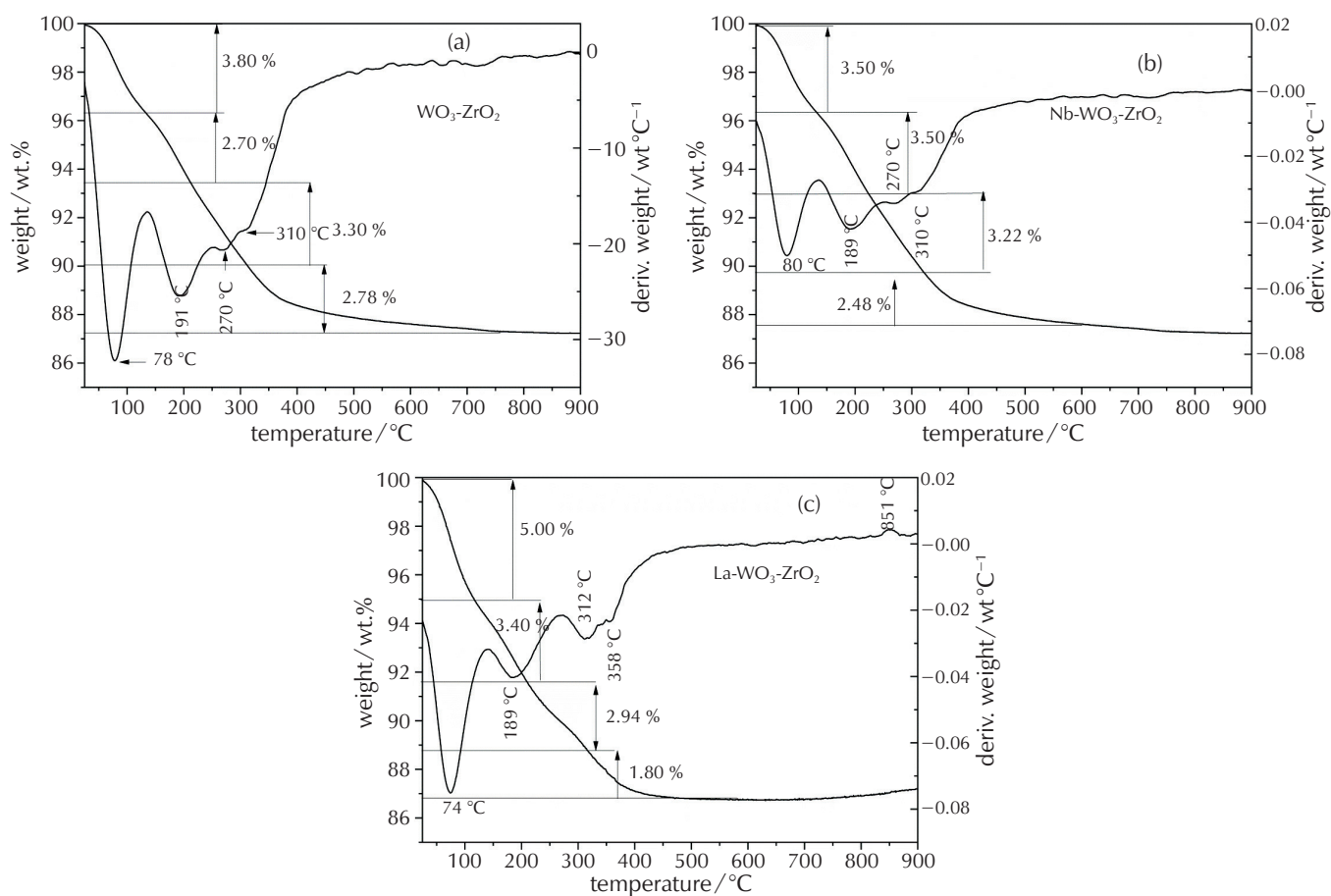


Fig. 2 – TG-DTA curves of the calcined catalysts (a) WZ, (b) 1 % NWZ, and (c) 1 % LWZ

takes place in the temperature range of 25–900 °C. The DTA curve in Fig. 2a for the calcined WZ catalyst shows four peaks in the temperature range of 25–350 °C resulting in a mass loss of 12.58 % of the total weight. Each mass loss was calculated between two consecutive peaks. The first two peaks corresponding to the release of physically adsorbed water (surface and intermediate layer); the third and fourth peaks could be due to the dehydroxylation.⁴⁵

The study of the 1 % NWZ material's behaviour in Fig. 2b shows two peaks at 80 and 189 °C due to the releasing of physically adsorbed water, with a total loss of 7 %. The two peaks appearing at higher temperatures (270 and 311 °C) could be related to the loss of the hydroxyl groups that make up the catalyst structure.⁴⁰

The plot in Fig. 2c indicates two stages of weight loss 1 % LWZ catalysts: one of 5 % by weight and another of 3.4 % below 200 °C, corresponding to the water desorption molecules adsorbed on the particles surface.

A total weight loss of 4.74 % by weight occurring at 312 and 358 °C corresponds to the sample dehydroxylation, as reported by *Jacom et al.*⁴⁵ The dehydroxylation suggests the formation of amorphous particles during synthesis, which were transformed into crystalline phases observed after annealing heat treatment.

After 500 °C, no more weight loss was detected for WZ and 1 % NWZ, except for 1 % LWZ catalysts where an exothermic peak at 840 °C was observed corresponding to the solid structure changes at high temperature.

For all samples, the pore size did not exceed 10 nm, thus, N_2 adsorption/desorption isotherms are type IV, characteristic of the adsorption of mesoporous solids. Both, the surface area by BET and the pore volume of WZ, calcined at 800 °C, attained 33 m² g⁻¹ and 0.13 cm³ g⁻¹, respectively (see Table 1). The addition of 1 % La slightly decreased both the surface area and the total pore volume. Adding 1 % Nb slightly increased the BET area from 33 to 35 m² g⁻¹. These changes in textural properties without modification of the zirconia structure are consistent with a physical effect of the promoter.

The pore size distributions (PSD) of different catalysts, shown in Fig. 3, were calculated by the BJH method. The dV/dD function of WZ exhibits a peak centred at about 3.86 nm and a larger one centred at around 8 nm for 1 % NWZ. The pore distribution for the 1 % LWZ material

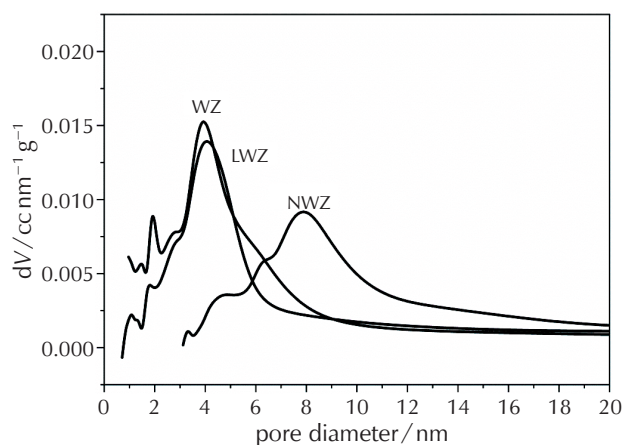


Fig. 3 – PSD for the calcined WZ, 1 % NWZ, and 1 % LWZ catalysts

shows a peak at 3.82 nm. According to our results, 1 % NWZ has the best textural properties.

In the isomerization of *n*-butane, Brønsted acid sites play a very important role. They are responsible for the protonation of the butene formed from the dehydrogenation of *n*-butane, and this reaction further leads to the formation of carbonic intermediates for the isomerization reaction.⁴⁶ The Brønsted acidity thus influences directly the rate of isomerization and coke formation of the catalyst in this reaction.

The acidity of our catalysts has been investigated by means of temperature-programmed-desorption (TPD). NH₃-TPD patterns of these catalysts are presented in Fig. 4. From the plots, it can be observed that there is no significant difference between the NH₃-TPD of WZ and 1 % NWZ catalysts. The total acidity was calculated from the NH₃ weight loss between 100 and 600 °C. For 1 % NWZ, the desorption temperature was at 240 °C. A large ammonia desorption peak was observed at 280 °C for WZ. The programmed desorption of 1 % LWZ was measured at 320 °C.

The NH₃ adsorption isotherms (Fig. 4) show clearly that the addition of niobium oxide led to a significant increase in ammonia adsorption. The acidity of 1 % NWZ was in the order of 283.53 μmol s⁻¹ g⁻¹. On the other hand, the addition of 1 % La had a negative effect on the amount of ammonia adsorbed (75.35 μmol s⁻¹ g⁻¹) representing the minimal acidity.

Table 1 – Acidity, textural, and structural properties of studied catalysts

Catalysts	$S_{\text{BET}}/\text{m}^2 \text{g}^{-1}$	Pore volume/cm ³ g ⁻¹	Pore size/nm	mZrO ₂ /tZrO ₂ ^a vol % / vol %	NH ₃ desorbed/μmol g ⁻¹
WZ	33	0.130	3.86	27/59	203.69
1 % NWZ	35	0.204	8.00	22/63	283.53
1 % LWZ	30	0.120	3.82	24/62	75.35

^a m: monoclinic phase of ZrO₂ and t: tetragonal phase of ZrO₂

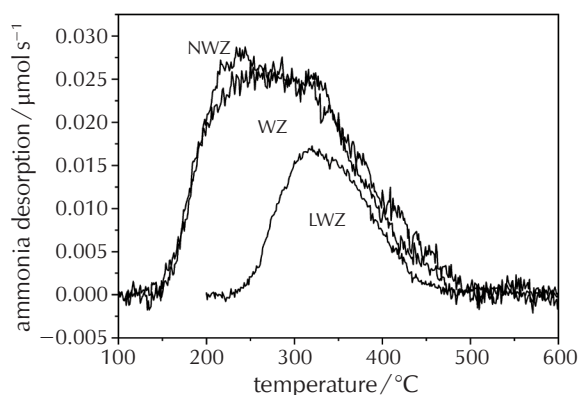


Fig. 4 – NH_3 -TPD profiles of the calcined WZ, 1 % NWZ, and 1 % LWZ catalysts

The high acidity of the 1 % NWZ catalyst can be attributed to the desorption rate of NH_3 between 100 and 600 °C. Above 600 °C, no ammonia was desorbed, it was completely removed. Mesoporous zirconia favours the formation of the strongest acid sites and at same time improves the total acid sites.

From the previous results, it is possible to associate the catalytic activity during the reaction of *n*-butane isomerization with structure and texture, acidity, or the presence of WO_3 crystallites.

Fig. 5 shows the catalytic activity for *n*-butane isomerization reaction in the presence of hydrogen for all catalysts. Under our reaction conditions, the main product in *n*-butane isomerization reaction was isobutene with minor products such as methane, ethane, propane, *n*-pentane, and isopentane. Activity and selectivity of *n*-butane isomerization can be temperature-dependent, as reported by Rossi et al.⁴⁷ Good reaction performances were obtained at 300 °C. The

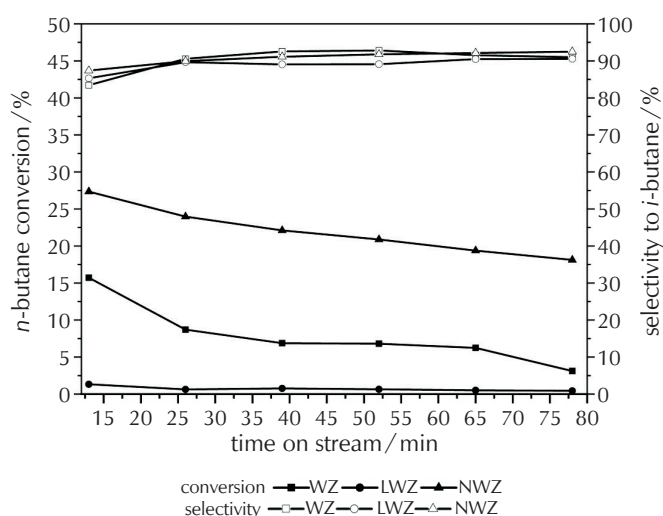


Fig. 5 – Conversion of *n*-butane, selectivity of *i*-butane as a function of reaction time on the calcined WZ, 1 % NWZ, and 1 % LWZ catalysts

promotion with 1 % Nb significantly improved the catalytic properties compared to pure WZ, and 1 % NWZ showed a higher *n*-butane conversion than 1 % LWZ.

For the most active catalyst (NWZ), 13 min was enough time to obtain a conversion rate of 27.34 %, and convert 1.32 % with the weakest active catalyst (LWZ). The conversion over WZ attained a stable conversion of 3.6 % after 78 min. A comparative study is presented in Table 2.

Table 2 – Comparative characteristics of WZ-based catalysts with different promoters in *n*-butane isomerization between our study and literature

Catalysts	Conversion ^{a,b} /%	Selectivity ^{a,c} /%	Refs.
1 % NWZ	27.34	92.34	our study
WZ	3.60	83.43	our study
1 % LWZ	1.32	85.30	our study
ZWPd	17.00	–	51
GWZ	26.20	81.50	43
FWZ	5.90	85.90	46
AWZ	6.50	89.38	50

^a Data taken after 5 min on stream at 300 °C; ^b Conversion of *n*-butane; ^c Selectivity to isobutane

The activity decreased with commissioning time, probably due to coke formation. We can observe that *n*-butane initial activity increased with the addition of 1 % Nb, and decreased with addition of 1 % La. Not much difference was observed in selectivity to *i*-C4 for promoted catalysts. Finally, the best conversion was achieved when the catalyst was promoted by 1 % Nb, which had the highest activity in the isomerization of *n*-butane. The good correlation obtained between acidity and catalytic activity indicates the strong influence of acidity and, in turn, the presence of tetragonal zirconia on the isomerization activity. These observations are consistent with those presented in the literature.^{33,48,49}

4 Conclusion

In the present study, it has been shown that the presence of niobium improves the catalytic stability and *n*-butane isomerization activity of WZ catalyst in the presence of H_2 at 300 °C. Under the same reaction conditions, catalytic activity of NWZ was found to be higher than WZ and LWZ catalysts. The addition of 1 % Nb to the WZ catalyst significantly increased the overall *n*-butane conversion (27.34 %) and selectivity to *i*-butane (92.34 %). It was found that 1 % NWZ catalyst exhibited the best structure (stable tetragonal structure) with $S_{\text{BET}} = 35 \text{ m}^2 \text{ g}^{-1}$ and NH_3 desorbed amount of $283.53 \text{ } \mu\text{mol g}^{-1}$. The high isomerization activity of the catalysts promoted by the addition of 1 % Nb in the presence of H_2 can be explained by assuming that the promoting effect of Nb is a combination of several factors, such as, (i) the acidity; (ii) the stability improvement of the

tetragonal structure; (iii) the crystal size effect of WO₃ on WZ surface, and (iv) the redox properties of W⁶⁺ improvement.

As perspectives of this study, we propose to increase the mass percentage of Nb and La promoters, and use cerium (Ce) on WO₃/ZrO₂ because their metallic properties will be modified (activation and dissociation of chemisorbed hydrogen, hydrogenation/dehydrogenation capacity, H₂-D₂ exchange). Moreover, hydrogen spillover, if existing on the targeted solids, could play a central role in enhancing isomerization catalytic activity.

ACKNOWLEDGEMENTS

We would like to express our gratitude to the Technical University of Berlin, in particular to professor Reinhard Schomäcker, and to the Algerian Ministry of Higher Education and Scientific Research through a scholarship for Z. Mohamed Seghir (PNE 2015/2016, Programme National Exceptionnel de Formation à l'Étranger) for financially supporting this research project.

References Literatura

- G. V. Echevskii, D. G. Aksenov, E. G. Kodenev, E. V. Ovchinnikova, V. A. Chumachenko, Activity of a Sulfated Zirconia Catalyst in Isomerization of *n*-Butane Fractions, *Pet. Chem.* **59** (2019) S101–S107, doi: <https://doi.org/10.1134/S0965544119130048>.
- J. M. Hidalgo, M. Zbuzek, R. Cerny, P. Jisa, Current uses and trends in catalytic isomerization, alkylation and etherification processes to improve gasoline quality, *Cent. Eur. J. Chem.* **12** (1) (2013) 1–13, doi: <https://doi.org/10.2478/s11532-013-0354-9>.
- K. P. de Jong, W. Bosch, T. D. B. Morgan, Developments in gasoline reformulation and the enhancement of refinery mtbe production, in: A. Frennet, J.-M. Bastin (Eds.), *Catalysis and Automotive Pollution Control III*, Stud. Surf. Sci. Catal. Vol. **96**, Elsevier Science, Amsterdam, 1995, pp. 15–32.
- M. E. Potter, J. J. M. Le Brocq, A. E. Oakley, E. B. McShane, B. D. Vandegheuchte, R. Raja, Butane Isomerization as a Diagnostic Tool in the Rational Design of Solid Acid Catalysts, *Catalysts* **10** (2020) 1099, doi: <https://doi.org/10.3390/catal10091099>.
- D. Seddon, Reformulated gasoline, opportunities for new catalyst technology, *Catal. Today* **15**(1) (1992) 1–21, doi: [https://doi.org/10.1016/0920-5861\(92\)80120-C](https://doi.org/10.1016/0920-5861(92)80120-C).
- M. Hino, K. Arata, Synthesis of solid superacid of tungsten oxide supported on zirconia and its catalytic action for reactions of butane and pentane, *J. Chem. Soc. Chem. Commun.* **18** (1988) 1259–1260, doi: <https://doi.org/10.1039/C39880001259>.
- I. Ullah, T. A. Taha, A. M. Alenad, I. Uddin, A. Hayat, A. Hayat, M. Sohail, A. Irfan, J. Khan, A. Palamanit, Platinum-alumina modified SO₄²⁻-ZrO₂/Al₂O₃ based bifunctional catalyst for significantly improved *n*-butane isomerization performance, *Surf. Interf.* **25** (2021) 101227, doi: <https://doi.org/10.1016/j.surfin.2021.101227>.
- J. M. Wulfers, F. C. Jentoft, Mechanism of *n*-butane skeletal isomerization on H-mordenite and Pt/H-mordenite, *J. Catal.* **330** (2015) 507–519, doi: <https://doi.org/10.1016/j.jcat.2014.12.035>.
- Y. Yamaguchi, Recent progress in solid superacid, *Appl. Catal.* **61** (1) (1990) 1–25, doi: [https://doi.org/10.1016/S0166-9834\(00\)82131-4](https://doi.org/10.1016/S0166-9834(00)82131-4).
- V. Nieminen, M. Kangas, T. Salmi, D. Y. Murzin, Kinetic Study of *n*-Butane Isomerization over Pt–H-Mordenite, *Ind. Eng. Chem. Res.* **44** (3) (2005) 471–484, doi: <https://doi.org/10.1021/ie049544q>.
- W. Hua, J. Sommer, Hydroisomerization of *n*-butane over sulfated zirconia catalysts promoted by alumina and platinum, *Appl. Catal. A-Gen.* **227** (1-2) (2002) 279–286, doi: [https://doi.org/10.1016/S0926-860X\(01\)00945-0](https://doi.org/10.1016/S0926-860X(01)00945-0).
- M. Hino, K. Arata, Synthesis of solid superacid catalyst with acid strength of H₀ ≤ –16.04, *J. Chem. Soc., Chem. Commun.* (1980) 851–852, doi: <https://doi.org/10.1039/C39800000851>.
- G. Xu Yan, A. Wang, I. E. Wachs, J. Baltrusaitis, Critical review on the active site structure of sulfated zirconia catalysts and prospects in fuel production, *Appl. Catal. A-Gen.* **572** (2019) 210–225, doi: <https://doi.org/10.1016/j.apcata.2018.12.012>.
- K. Tanabe, H. Hattori, T. Yamaguchi, Surface properties of solid superacids, *Crit. Rev. Surf. Chem.* **1** (1990) 1–25.
- Z. Hong, K. B. Fogash, J. A. Dumesic, Reaction kinetic behavior of sulfated-zirconia catalysts for butane isomerization, *Catal. Today* **51** (1999) 269–288, doi: [https://doi.org/10.1016/S0920-5861\(99\)00050-4](https://doi.org/10.1016/S0920-5861(99)00050-4).
- V. Adeeva, J. de Haan, J. Janchen, G. Lei, Acid Sites in Sulfated and Metal-Promoted Zirconium Dioxide Catalysts, *J. Catal.* **151** (2) (1995) 364–372, doi: <https://doi.org/10.1006/jcat.1995.1039>.
- C.-Y. Hsu, C. R. Heimbuch, C. T. Armes, B. C. Gates, A Highly Active Solid Superacid Catalyst for *n*-Butane Isomerization: a Sulfated Oxide Containing Iron, Manganese and Zirconium, *J. Chem. Soc. Chem. Commun.* **22** (1992) 1645–1646, doi: <https://doi.org/10.1039/C39920001645>.
- T. Loften, N. S. Gnep, M. Guisnet, E. A. Belkkan, Iron and manganese promoted sulfated zirconia: acidic properties and *n*-butane isomerization activity, *Catal. Today* **100** (3-4) (2005) 397–401, doi: <https://doi.org/10.1016/j.cattod.2004.09.071>.
- P. Wang, Y. Yue, T. Wang, X. Bao, Alkane isomerization over sulfated zirconia solid acid system, *Int. J. Energy Res.* **44** (5) (2020) 3270–3294, doi: <https://doi.org/10.1002/er.4995>.
- P. Wang, J. Zhang, G. Wang, C. Li, C. Yang, Nature of active sites and deactivation mechanism for *n*-butane isomerization over alumina-promoted sulfated zirconia, *J. Catal.* **338** (2016) 124–134, doi: <https://doi.org/10.1016/j.jcat.2016.02.027>.
- G. Larsen, E. Lotero, R. D. Parra, L. M. Petkovic, H. S. Silva, S. Raghavan, Characterization of palladium supported on sulfated zirconia catalysts by DRIFTS, XAS and *n*-butane isomerization reaction in the presence of hydrogen, *Appl. Catal. A-Gen.* **130** (1995) 213–226, doi: [https://doi.org/10.1016/0926-860X\(95\)00117-4](https://doi.org/10.1016/0926-860X(95)00117-4).
- J. C. Yori, J. M. Parera, *n*-Butane isomerization on metal-promoted sulfated zirconia, *Appl. Catal. A-Gen.* **147** (1) (1996) 145–157, doi: [https://doi.org/10.1016/S0926-860X\(96\)00214-1](https://doi.org/10.1016/S0926-860X(96)00214-1).
- A. Jatia, C. Chang, J. D. MacLeod, T. Okubo, M. E. Davis, ZrO₂ promoted with sulfate, iron and manganese: a solid superacid catalyst capable of low temperature *n*-butane isomerization, *Catal. Lett.* **25** (1994) 21–28, doi: <https://doi.org/10.1007/BF00815411>.
- X.-R. Chen, C.-L. Chen, N.-P. Xu, C.-Y. Mou, Al- and Ga-pro-

- moted WO_3/ZrO_2 strong solid acid catalysts and their catalytic activities in *n*-butane isomerization, *Catal. Today* **93-95** (2004) 129–134, doi: <https://doi.org/10.1016/j.cattod.2004.06.030>.
25. M. Scheithauer, R. K. Grasselli, H. Knözinger, Genesis and Structure of WO_x/ZrO_2 Solid Acid Catalysts, *Langmuir* **14** (1998) 3019–3029, doi: <https://doi.org/10.1021/la971399g>.
 26. N. Naito, N. Katada, M. Niwa, Tungsten Oxide Monolayer Loaded on Zirconia: Determination of Acidity Generated on the Monolayer, *J. Phys. Chem. B.* **103** (34) (1999) 7206–7213, doi: <https://doi.org/10.1021/jp9906381>.
 27. S. De Rossi, G. Ferraris, M. Valigi, D. Gazzoli, WO_x/ZrO_2 catalysts: Part 2. Isomerization of *n*-butane, *Appl. Catal. A-Gen.* **231** (1-2) (2002) 173–184, doi: [https://doi.org/10.1016/S0926-860X\(02\)00049-2](https://doi.org/10.1016/S0926-860X(02)00049-2).
 28. K. Arata, Preparation of Solid Superacid Catalysts, *J. Japan Pet. Inst.* **39** (1996) 185–193, doi: <https://doi.org/10.1627/jpi1958.39.185>.
 29. D. G. Barton, S. L. Soled, G. D. Meitzner, G. A. Fuentes, E. Iglesia, Structural and Catalytic Characterization of Solid Acids Based on Zirconia Modified by Tungsten Oxide, *J. Catal.* **181** (1) (1999) 57–72, doi: <https://doi.org/10.1006/jcat.1998.2269>.
 30. S. R. Vaudagna, S. A. Canavese, R. A. Comelli, N. S. Figoli, Platinum supported $\text{WO}_x\text{-ZrO}_2$: Effect of calcination temperature and tungsten loading, *Appl. Catal. A-Gen.* **168** (1998) 93–111, doi: [https://doi.org/10.1016/S0926-860X\(97\)00343-8](https://doi.org/10.1016/S0926-860X(97)00343-8).
 31. G. Larsen, E. Lotero, S. Raghavan, R. D. Parra, C. A. Querini, A study of platinum supported on tungstated zirconia catalysts, *Appl. Catal. A-Gen.* **139** (1996) 201–211, doi: [https://doi.org/10.1016/0926-860X\(95\)00330-4](https://doi.org/10.1016/0926-860X(95)00330-4).
 32. C.-L. Chen, T. Li, S. Cheng, N.-P. Xu, C.-Y. Mou, Catalytic Behavior of Alumina-Promoted Sulfated Zirconia Supported on Mesoporous Silica in Butane Isomerization, *Catal. Lett.* **78** (2002) 223–229, doi: <https://doi.org/10.1023/A:1014908618311>.
 33. R. A. Boyse, E. I. Ko, Crystallization Behavior of Tungstate on Zirconia and Its Relationship to Acidic Properties, *J. Catal.* **171** (1997) 191–207, doi: <https://doi.org/10.1006/jcat.1997.1761>.
 34. A. H. Karima, S. Triwahyono, A. Abdul Jalilb, H. Hattoric, WO_3 monolayer loaded on ZrO_2 : Property–activity relationship in *n*-butane isomerization evidenced by hydrogen adsorption and IR studies, *Appl. Catal. A-Gen.* **433-434** (2012) 49–57, doi: <https://doi.org/10.1016/j.apcata.2012.04.039>.
 35. N. Vaidyanathan, D. M. Hercules, M. Houalla, Surface characterization of WO_3/ZrO_2 catalysts, *Anal. Bioanal. Chem.* **373** (2002) 547–554, doi: <https://doi.org/10.1007/s00216-002-1386-8>.
 36. E. Iglesia, D. G. Barton, S. L. Soled, S. Miseo, J. E. Baumgartner, W. E. Gates, G. A. Fuentes, G. D. Meitzner, Selective isomerization of alkanes on supported tungsten oxide acids, in: J. W. Hightower, W. N. Delgass, E. Iglesia, A. T. Bell (Eds.), Proceedings of the 11th International Congress on Catalysis, 40th Anniversary, *Stud. Surf. Sci. Catal.* Vol. 101, Elsevier Science, Amsterdam, 1996, pp. 533–542, doi: [https://doi.org/10.1016/S0167-2991\(96\)80264-3](https://doi.org/10.1016/S0167-2991(96)80264-3).
 37. R. Ponnusamy, A. Gangan, B. Chakraborty, C. S. Rout, Tuning the pure monoclinic phase of WO_3 and $\text{WO}_3\text{-Ag}$ nanostructures for non-enzymatic glucose sensing application with theoretical insight from electronic structure simulations, *J. Appl. Phys.* **123** (2018) 024701, doi: <https://doi.org/10.1063/1.5010826>.
 38. A. Martinez, G. Prieto, M. A. Arribas, P. Concepción, Hydroconversion of *n*-hexadecane over $\text{Pt}/\text{WO}_x\text{-ZrO}_2$ catalysts prepared by a PVA-template coprecipitation route: The effect of tungsten surface coverage on activity and selectivity, *Appl. Catal. A-Gen.* **309** (2006) 224–236, doi: <https://doi.org/10.1016/j.apcata.2006.05.010>.
 39. Z. Chen, Relation microstructure et propriété mécanique des films de ZrO_2 obtenus par MOCVD. Doctoral thesis, Université Paris Sud, Paris, 2011.
 40. F. Di Gregorio, V. Keller, Activation and isomerization of hydrocarbons over WO_3/ZrO_2 catalysts: I. Preparation, characterization, and X-ray photoelectron spectroscopy studies, *J. Catal.* **225** (2004) 45–55, doi: <https://doi.org/10.1016/j.jcat.2004.03.023>.
 41. J. C. Yori, C. R. Vera, J. M. Parera, *n*-Butane isomerization on tungsten oxide supported on zirconia, *Appl. Catal. A-Gen.* **163** (1997) 165–175, doi: [https://doi.org/10.1016/S0926-860X\(97\)00140-3](https://doi.org/10.1016/S0926-860X(97)00140-3).
 42. Y.-Y. Huang, B.-Y. Zhao, Y.-C. Xie, Modification of sulfated zirconia by tungsten oxide: Acidity enhancement and structural characterization, *Appl. Catal. A-Gen.* **171** (1998) 75–83, doi: [https://doi.org/10.1016/S0926-860X\(98\)00073-8](https://doi.org/10.1016/S0926-860X(98)00073-8).
 43. X.-R. Chen, C.-L. Chen, N.-P. Xu, S. Han, C. Y. Mou, Ga-Promoted Tungstated Zirconia Catalyst for *n*-Butane Isomerization, *Catal. Lett.* **85** (2003) 177–182, doi: <https://doi.org/10.1023/A:1022137612328>.
 44. W. Stichert, F. Schüth, Synthesis of Catalytically Active High Surface Area Monoclinic Sulfated Zirconia, *J. Catal.* **174** (2) (1998) 242–245, doi: <https://doi.org/10.1006/jcat.1998.1962>.
 45. M. A. Cortés-Jácome, J. A. Toledo-Antonio, H. Armendáriz, I. Hernández, X. Bokhimiz, Solid Solutions of WO_3 into Zirconia in $\text{WO}_3\text{-ZrO}_2$ Catalysts, *J. Solid State Chem.* **164** (2002) 339–344, doi: <https://doi.org/10.1006/jssc.2001.9488>.
 46. S.-T. Wong, T. Li, S. Cheng, J.-F. Lee, C.-Y. Mou, Platinum- and iron-doubly promoted tungstated zirconia catalyst for *n*-butane isomerization reaction, *Appl. Catal. A-Gen.* **296** (2005) 90–99, doi: <https://doi.org/10.1016/j.apcata.2005.08.004>.
 47. M. Valigi, D. Gazzoli, I. Pettiti, G. Mattei, S. Colonna, S. De Rossi, J. Ferraris, WO_x/ZrO_2 catalysts: Part 1. Preparation, bulk and surface characterization, *Appl. Catal. A-Gen.* **231** (1-2) (2002) 159–172.
 48. M. Scheithauer, T. K. Cheung, R. E. Jentoft, R. K. Grasselli, B. C. Gates, H. Knözinger, Characterization of WO_x/ZrO_2 by Vibrational Spectroscopy and *n*-Pentane Isomerization Catalysis, *J. Catal.* **180** (1998) 1–13, doi: <https://doi.org/10.1006/jcat.1998.2237>.
 49. V. Adeeva, H.-Y. Liu, B.-Q. Xu, W. M. H. Sachtler, Alkane isomerization over sulfated zirconia and other solid acids, *Topics Catal.* **6** (1998) 61–67, doi: <https://doi.org/10.1023/A:1019114406219>.
 50. S.-T. Wong, T. Li, S. Cheng, J.-F. Lee, C.-Y. Mou, Aluminum-promoted Tungstatedzirconia catalyst in *n*-butane isomerization reaction, *J. Catal.* **215** (2003) 45–56, doi: [https://doi.org/10.1016/S0021-9517\(02\)00176-8](https://doi.org/10.1016/S0021-9517(02)00176-8).
 51. M. Occhiuzzi, D. Cordischi, S. De Rossi, G. Ferraris, D. Gazzoli, M. Valigi, Pd-promoted WO_x/ZrO_2 catalysts: Characterization and catalytic activity for *n*-butane isomerization, *Appl. Catal. A-Gen.* **351** (2008) 29–35, doi: <https://doi.org/10.1016/j.apcata.2008.08.025>.

SAŽETAK

Studija izomerizacije *n*-butana na kiselim WO₃/ZrO₂ katalizatorima potaknutim niobijem i lantanom: aktivnost izomerizacije *n*-butana

Zahira Mohamed Seghir,^{a*} Mhamed Djennad,^a Reinhard Schomäcker^b i Mouffok Redouane Ghezzer^c

Potreba za ekološki prihvatljivim katalizatorima primjenjivim za izomerizaciju alkana potaknuo je istraživanje sustava volframat-cirkonij (WZ). Ovaj rad ispituje aktivnost i selektivnost lantanom i niobijem potaknutih WZ katalizatora. U studiji je ispitana primjena WZ katalizatora potaknutih dodatkom 1 % lantana (1 % LWZ), odnosno 1 % niobija (1 % NWZ), u izomerizaciji *n*-butana u prisutnosti vodika. Karakterizacija je provedena različitim metodama: fizisorpcijom dušika, temperaturno programiranom desorpcijom amonijaka, termogravimetrijskom analizom i rendgenskom difrakcijskom analizom. Katalitička aktivnost i selektivnost znatno su poboljšani dodatkom 1 % niobija. Redoks-proces u katalizatoru koji je sadržavao niobij odigrao je glavnu ulogu osiguravajući najviše kiselih mjesta (283,53 μmol g⁻¹) s odgovarajućom energijom aktivacije za preslagivanje *n*-butana. Konverzija *n*-butana (27,34 %) i selektivnost prema *i*-butanu (92,34 %) kod NWZ katalizatora bili su znatno veći nego kod WZ i LWZ katalizatora. Eksperimentalna istraživanja ukazuju učinkovitije poticanje dodatkom niobija u usporedbi s lantanom.

Ključne riječi

Sustav volframat-cirkonij, izomerizacija *n*-butana, niobij, lantan, kiselost

^a Laboratory of Structure, Elaboration and Application of Molecular Materials, SEA2M Department of Process Engineering, University Abdelhamid Ibn Badis, Mostaganem, Alžir

^b Department of Chemistry, Technical University Berlin, StraÙe des 17. Juni 124, 10 623 Berlin, Njemačka

^c Laboratory of Science and Technical Environment and Valorization, Department of Process Engineering, University Abdelhamid Ibn Badis, Mostaganem, Alžir

Izvorni znanstveni rad
Prispjelo 5. prosinca 2021.
Prihvaćeno 11. veljače 2022.